A Visual Interaction Framework for Dimensionality Reduction Based Data Exploration

Marco Cavallo
IBM Research
mcavall@us.ibm.research

Çağatay Demiralp
IBM Research
cagatay.demiralp@us.ibm.research

ABSTRACT

Dimensionality reduction is a common method for analyzing and visualizing high-dimensional data. However, reasoning dynamically about the results of a dimensionality reduction is difficult. Dimensionality-reduction algorithms use complex optimizations to reduce the number of dimensions of a dataset, but these new dimensions often lack a clear relation to the initial data dimensions, thus making them difficult to interpret.

Here we propose a visual interaction framework to improve dimensionality-reduction based exploratory data analysis. We introduce two interaction techniques, forward projection and backward projection, for dynamically reasoning about dimensionally reduced data. We also contribute two visualization techniques, prolines and feasibility maps, to facilitate the effective use of the proposed interactions.

We apply our framework to PCA and autoencoder-based dimensionality reductions. Through data-exploration examples, we demonstrate how our visual interactions can improve the use of dimensionality reduction in exploratory data analysis.

Author Keywords

Dimensionality reduction; interaction; bidirectional binding; visual embedding; forward projection; backward projection; PCA; autoencoder; deep learning; proline; feasibility map; exploratory data analysis; what-if analysis; Praxis.

INTRODUCTION

Dimensionality reduction (DR) is widely used for exploratory data analysis (EDA)[57] of high-dimensional datasets. DR algorithms automatically reduce the number of dimensions in data while maximally preserving structures, typically quantified as similarities, correlations or distances among data points [58]. This makes visualization of the data possible using conventional spatial techniques. For instance, analysts generally use scatter plots to visualize the data after reducing the number of dimensions to two, encoding the reduced dimensions in a two-dimensional position.

CHI 2018, April 21–26, 2018, Montreal, QC, Canada

ISBN 978-1-4503-5620-6/18/04…$15.00
DOI: https://doi.org/10.1145/3173574.3174209

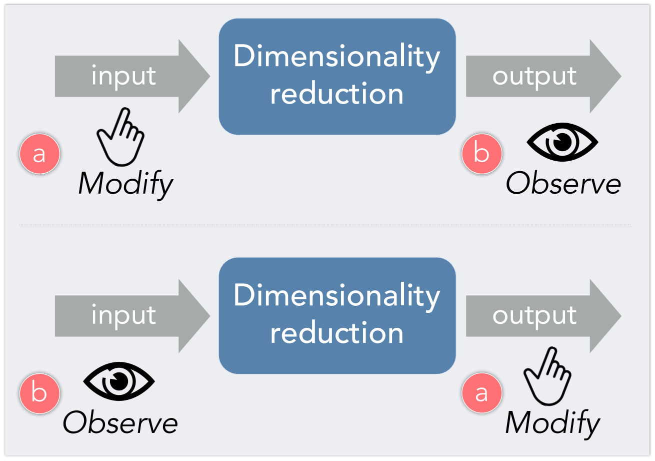

Figure 1: Better interaction with DR models to improve DR-based exploratory analysis? Two complementary affordances can help: (Top) Modify the input to the model first and then see how the model output changes. (Bottom) Modify the model output first and then see how the input needs to change (be synthesized) so that the DR model generates the user-induced output. These two affordances can improve DR-based exploratory analysis by concurrently facilitating model understanding and what-if analysis.

DR Challenges: DR methods are driven by complex numerical optimizations, which makes dynamic reasoning about DR results difficult. Dimensions derived by these methods generally lack clear, easy-to-interpret mappings to the original data dimensions. Data analysts with limited experience in DR have in difficulty in interpreting the meaning of the projection axes and the position of scatter plot nodes [10, 51]: 'What do the axes mean?" is frequently asked by users looking at scatter plots whose points (nodes) correspond to dimensionally reduced data. As a result, analysts treat DR methods as black boxes and often rely on off-the-shelf routines in their toolset for computation and visualization. Indeed, most scatter-plot visualizations of dimensionally reduced data are viewed as static images. One reason is that tools for computing and plotting these visualizations, such as Python, R, and Matlab, have few interactive exploration functionalities. Another reason is that few interaction and visualization techniques go beyond brushing-and-linking or cluster-based coloring to allow dynamic reasoning with DR visualizations.

However, the ability not only to probe the results of a DR model but also actively to tinker with them is important for a model-based EDA, as experimentation is essential to data exploration [57]. Enabling an analyst to run various input and output scenarios and see how the underlying DR model—coupled with data—responds can facilitate model understanding and is a prerequisite for what-if analysis.

Improving DR-Based Exploratory Analysis: In response, we propose a visual interaction framework to improve DR-based data exploration. To this end, we introduce two interaction techniques, *forward projection* and *backward projection*, to help analysts dynamically explore and reason about scatter plot representations of dimensionally reduced data. We also contribute two visualization techniques, *prolines* and *feasibility map*, to facilitate the effective use of the proposed interactions.

The underlying idea (Figure 1) of our framework is that the ability to induce *change* and observe the *effects* of that change is essential for reasoning with DRs or any black-box models (more on this in Discussion). Forward projection enables an analyst to interactively change data attributes input to a DR routine and observe the effects in the output. Backward projection complements forward projection by letting the analyst make hypothetical changes to the output, the attributes of new dimensions, and observe which changes in the input attribute values would produce the hypothesized changes in the output. These affordances are useful for running what-if scenarios as well as understanding the underlying DR process.

Contributions: Our high-level contribution is 1) a new framework that aims to enable users to dynamically change the input and output of DRs and observe the effects of these changes. The design of the visual interactions that operationalize the underlying purpose of the framework also has novel attributes. These contributions include 2) the forward projection interaction using out-of-sample (OOS) extension, 3) the proline visualization along with its visual and interactive affordances, 4) the backward projection interaction with interactive user constraints, and 5) the feasibility map visualization.

Any DR algorithm with fast OOS extension (extrapolation) and inversion methods can be plugged in our framework. We apply the framework to PCA (principal component analysis) and autoencoder-based dimensionality reductions and demonstrate how it improves DR-based exploratory analysis.

Next we discuss related work and then introduce our framework interactions. We then present applications to PCA and autoencoder and give exploratory analysis examples, and then elaborate on the scalability and accuracy of our methods. Then we discuss how the current model extends to black-box models at large, such as deep learning models, and how changes in model development practices can help improve explorability and interpretability of black-box models. We conclude by summarizing our contributions and reflecting on the importance of EDA tools that support interactive experimentation.

RELATED WORK

Our work builds on prior research in direct manipulation and auxiliary visual encoding in scatter plots of dimensionality reductions (DRs).

Direct Manipulation in DR

Direct manipulation has a long history in human-computer interaction [8, 31, 56] and visualization research (e.g. [52]). Direct manipulation techniques aim to improve user engagement by minimizing the *perceived* distance between the interaction source and the target object [27].

Developing direct manipulation interactions to guide DR formation and modify the underlying data is a focus of prior research [11, 19, 23, 28, 29, 61]. For example, X/GGvis [11] supports changing the weights of dissimilarities input to the MDS stress function along with the coordinates of the embedded points in order to guide the projection process. Similarly, iPCA [28] enables users to interactively modify the weights of data dimensions in computing projections. Endert *et al.* [20] apply similar ideas to additional dimensionality-reduction methods while incorporating user feedback through spatial interactions in which users can express their intent by dragging points in the plane.

Earlier work also uses direct manipulation to modify data through DR visualizations in order to support, e.g., exploratory analysis [28], multivariate network manipulation [59], exploration of trajectory clusters [50], movement trace analysis [16], and feature transformation [43]. Our work here aims to facilitate DR-based exploratory analysis. Akin to forward projection and unconstrained backward projection techniques, iPCA [28] enables interactive forward and backward projections for PCA-based DRs. However, iPCA recomputes full PCAs for each forward and backward projection, and these can suffer from jitter and scalability issues. Using out-of-sample extrapolation [6, 58], our forward projection avoids re-running dimensionality reduction algorithms. Unlike iPCA, we also enable users to interactively define constraints on feature values and perform constrained backward projection.

We refer readers to a recent survey [49] for an exhaustive discussion of prior work on visual interaction with dimensionality reduction.

Visualization in DR Scatter Plots

Prior work incorporates various visualizations in planar scatter plots of DRs in order to improve the user experience [3, 14, 18, 22, 28, 38, 55]. Since low-dimensional projections are generally lossy representations of the high-dimensional data relations, it is useful to convey both overall and per-point dimensionality-reduction errors to users when desired. Researchers visualized errors in DR scatter plots using Voronoi diagrams [3, 38] and corrected (undistorted) the errors by adjusting the projection layout with respect to the examined point [14, 55].

Biplot was introduced [22] to visualize the magnitude and sign of a data attribute's contribution to the first two or three principal components as line vectors in PCA. Biplots are computed using singular-value decomposition, regardless of the actual DR used, assuming the underlying DR is linear and the data matrices needed to compute the decomposition are accessible.

Closest to our prolines are the *enhanced biplots* introduced by Coimbra *et al.* [15]. Enhanced biplots aim to extend biplots to nonlinear DRs and assume only access to the projection function of a DR, thus sharing similar assumptions and generaliza-

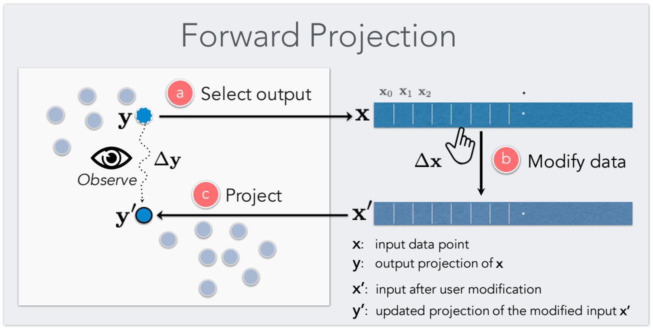

Figure 2: Forward projection enables users to: (a) select any data point instance $\mathbf{x}$ that is input to a DR, (b) interactively change its high-dimensional feature values, and (c) observe the change $\Delta\mathbf{y}$ in the point's two-dimensional projection.

tion properties with prolines. Similarly to a proline construction, each axis of an enhanced biplot is constructed by connecting the projections of points sampled on the range of the corresponding data attribute. However, prolines differ from enhanced biplots in a few aspects. Both enhanced and classical biplots visualize how projections (reduced dimensions) change on average with changing attribute values, whereas Prolines are computed for each data and attribute and visualize projection changes locally for each data point. In this sense, prolines complement enhanced biplots by constructing local axes of projection change with respect to data attributes. To construct an attribute axis, enhanced biplots use values regularly sampled on the attribute's range with a sampling rate uniform across axes, while keeping the remaining attributes constant at their average values. On the other hand, we modulate the sampling rate with attribute variances and decorate prolines with marks to communicate distributional characteristics of the underlying data point. More crucially, prolines differ from this earlier work in being interactive visual signifiers that dynamically facilitate user interactions.

Stahnke *et al.* [55] use a grayscale map to visualize how a single attribute value changes between data points in DR scatter plots. We introduce the feasibility map, a grayscale map, to visualize the feasible regions in the constrained backward projection interaction.

We have presented our work at different stages of its development at two workshops. We introduced an initial version as part of Clustrophile, an exploratory visual clustering analysis tool [18]. We then presented our revised visual interactions integrated with Praxis, an interactive DR-based exploratory analysis tool, in a dedicated draft [12]. Here we give a unified treatment of our work by formalizing it under a framework. The current work also demonstrates the use of our visual interactions through several new data-exploration examples and provides a new discussion that relates the applicability of our framework to black-box models, particularly deep learning models, at large.

VISUAL INTERACTIONS

We now discuss the interactions and the related visualizations in our framework.

Forward Projection

Forward projection enables users to interactively change the feature values of a data input $\mathbf{x}$ and observe how these hypothesized changes in data modify the current projected location $\mathbf{y}$ (Figure 2).

We compute forward projections using out-of-sample (OOS) extension (or extrapolation) [58]. OOS extension is the projection of a new data point into an existing dimensionality reduction (DR) using only the properties of the already computed DR. It is thus conceptually equivalent to testing a trained machine-learning model with data that was not part of the training set. Most common DR methods have OOS extension algorithms with desirable accuracy properties [6].

We propose using OOS extension as opposed to re-running the DR for two basic reasons. The first is scalability: OOS computation is generally much faster than re-running the dimensionality reduction, and speed is critical in sustaining the interactive experience. The second is preserving the constancy of scatter plot representations [5]. For example, re-running (training) a dimensionality-reduction algorithm with a new data sample added can significantly alter the two-dimensional scatter plot of the dimensionally reduced data, even though all the original inter-datapoint similarities may remain unchanged. With OOS, forward projection animations change the position of only the point attributes that the user interactively modifies.

Prolines: Visualizing Forward Projections

Forward projection provides a scalable interaction to change the attributes of a data instance and see how the dimensionality reduction changes. We introduce prolines to let users see in advance what forward projection paths look like for each data point and feature. Through prolines, an analyst can see what directly start exploring data without considering forward projections exhaustively.

Prolines visualize forward projection paths using regularly sampled values for each feature and data point (Figures 3). Let $\mathbf{x}_i$ be the value of the ith feature for the data point $\mathbf{x}$. We first compute the mean μ_i, standard deviation σ_i, minimum $\min_i$ and maximum $\max_i$ values for the feature in the dataset and devise a range $I = [\min_i, \max_i]$. We then iterate over the range with step size $c\sigma_i$, compute the forward projections as discussed above, and then connect them as a path.

In addition to providing an advance snapshot of forward projections, a proline also conveys the relationship between the feature distribution and the projection space. To that end, we display along each proline a small light-blue circle indicating the position that the data point would assume if it had a feature value corresponding to the mean of its distribution; similarly, we display two small arrows indicating a variation of one standard deviation (σ_i) from the mean (μ_i). The segment identified by the range $[\mu_i - \sigma_i, \mathbf{x}_i + \sigma_i]$ is highlighted and further divided into two segments. The green segment shows the positions that the data point would assume if its feature value increased; the red one indicates a decreasing value. This enables users to infer the relationship between the feature space and the direction of change in the projection space.

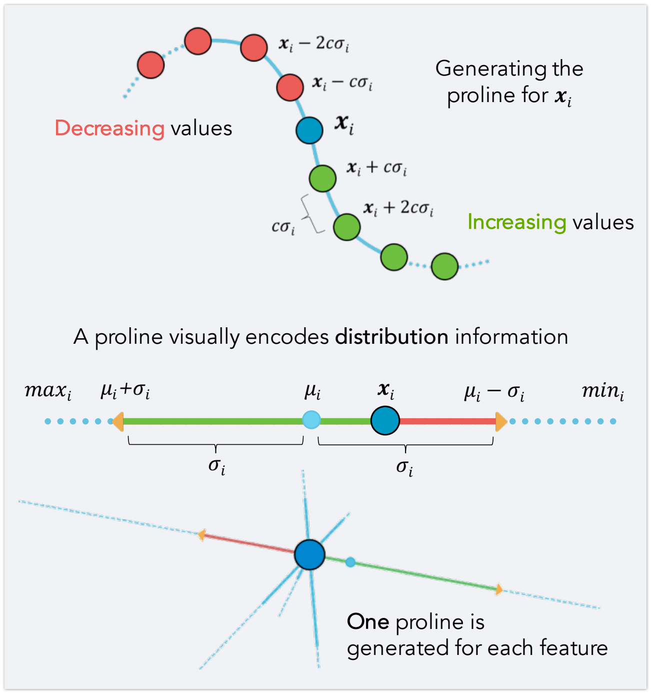

Figure 3: Proline construction. For a given dimension (feature) x_i of a point **x** in a dataset, we construct a proline by connecting the forward projections of data points regularly sampled from a range of **x** values, where all features are fixed but x_i varies. A proline also encodes the forward projections for the x_i values in $[\mu_i - \sigma_i, \mu_i + \sigma_i]$ with thick green and red line segments, providing a basic directional statistical context. μ_i is the mean of the ith dimension in the dataset, the green segment represents forward projections for x_i values in $[x_i, \mu_i + \sigma_i]$, and the red segment represents x_i values in $[\mu_i - \sigma_i, x_i]$.

Backward Projection

Backward projection complements the forward projection interaction by enabling a user to interactively change output attributes and observe how the input attributes change as the DR routine produces the user-induced output. Consider the following scenario: a user looks at a projection and, seeing a cluster of points and a single point projected far from this group, asks what changes in the feature values of the outlier point would bring it near the cluster. Now the user can play with different dimensions using forward projection interactions to move the current projection of the outlier point near the cluster. It would be more natural, however, to move the point directly and observe the change.

Back or backward projection maps a low-dimensional data point back into the original high-dimensional data space. For linear DRs, back projection is typically done by applying the inverse of the learned linear DR mapping. For nonlinear DRs, earlier research proposed DR-specific backward-projection techniques. For example, iLAMP [2] introduces a back-projection method for LAMP [30] using local neighborhoods and demonstrates its viability over synthetic datasets [2]. Researchers also investigated general backward-projection methods based on radial basis functions [1, 44], treating backward projection as an interpolation problem. Autoencoders [26], neural-network-based DR models, are a promising approach to computing backward projections. An autoencoder model with multiple hidden layers can learn a nonlinear dimensionality-reduction function (encoding) as well as the corresponding backward projection (decoding) as part of the DR process.

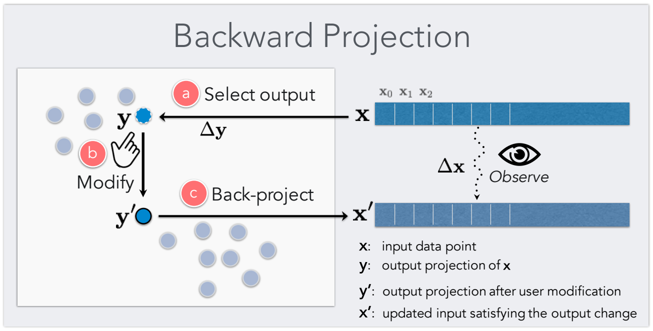
Backward Projection
a Select output
y
Δy
x
x_0 x_1 x_2
b
Modify
c Back-project
y′
x′
Δx
Observe
x: input data point
y: output projection of x
y′: output projection after user modification
x′: updated input satisfying the output change

Figure 4: Backward projection enables users to: (a) select any node corresponding to the two-dimensional projection of a data point **x**, (b) move the node arbitrarily in the plane, and (c) observe the change $\Delta\mathbf{x}$ in the point's high-dimensional feature values.

We propose both *constrained* and *unconstrained* backward projection interactions. Constrained backward projection enhances what-if analysis by letting analysts semantically regulate the mapping into unprojected high-dimensional data space. For example, we don't expect an Age field to be negative or greater than 200, even though such a value can be a more optimal solution in an unconstrained backward projection scenario. DRs are many-to-one functions (more on this in Supplementary Material) in general, and hence inverting them is an underdetermined problem that benefits from regularization. Therefore, in addition to augmenting what-if analysis, the ability to define constraints over a back projection can also ease the computational burden by restricting the search space for a feasible solution.

It is important to note that, since more than one data point in the multidimensional space can project to the same position, forward and backward projections may not always correspond. For this reason, we add to our prolines visualization a set of *projection marks* (Figure 7b) indicating the current value for each feature while the user performs backward projection. At the same time, dragging a data point highlights the green or red segment of each proline based on the increase or decrease of each feature, showing which dimensions are correlated. By combining forward projection paths and backward projection, the user can infer how fast each value is changing in relation to its feature distribution.

Feasibility Map: Visualizing Constraint Satisfaction

We propose the feasibility map visualization as a way quickly to see the feasible space determined by a given set of constraints. Instead of manually checking if a position in the projection plane satisfies the desired range of values (considering both equality and inequality constraints), one would like to know

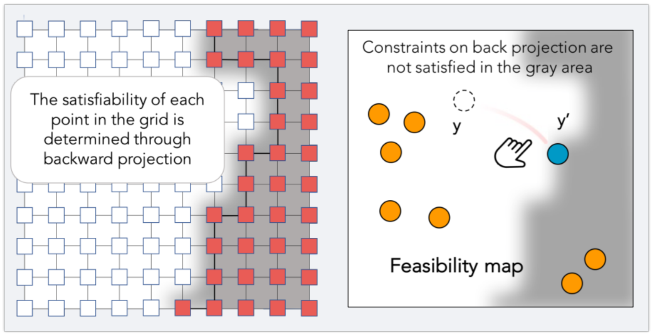
The satisfiability of each point in the grid is determined through backward projection
Constraints on back projection are not satisfied in the gray area
y
y'
Feasibility map

Figure 5: Feasibility map. The feasibility map is constructed by sampling the projection plane through constrained backward projection and then verifying the existence of each solution (left). The darker area of the map, computed through interpolation, corresponds to the positions of the plane that would break the constraints for the specified data point (right).

in advance which regions of the plane correspond to admissible solutions. In this sense, a feasibility map is a conceptual generalization of prolines to the constrained backward projection interaction.

To generate a feasibility map, we sample the projection plane on a regular grid and evaluate the feasibility at each grid point based on the constraints imposed by the user, obtaining a binary mask over the projection plane. We render this binary mask over the projection as an interpolated grayscale heatmap in which darker areas indicate infeasible planar regions (Figure 5). With accuracy determined by the grid resolution, the user can see which areas a data point can assume in the projection plane without breaking the constraints. In backward projection, if a data point is dragged to a position that does not satisfy a constraint, its color and the color of its corresponding projection marks turn to black. If the user drops the data point in an infeasible position, the point is automatically moved through animation back to the last feasible position to which it was dragged.

APPLICATIONS

We apply our framework to PCA (principal component analysis) and autoencoder-based dimensionality reductions (DRs) and demonstrate how it improves DR-based exploratory analysis. We choose PCA and autoencoder because they respectively cover linear and nonlinear DR cases and have effective extension and inversion methods. PCA, among the most frequently used DR methods, is effective for rapid initial exploratory analysis and requires no parameter tuning. Note that the framework can be applied to any DR algorithm with fast inversion and out-of-sample (OOS) extension methods. As their fast inversion and extension methods become available, the framework can easily applied to other popular DR methods such as t-SNE [41].

In what follows we first briefly introduce Praxis, a new tool for interactive DR-based data analysis that integrates our framework interactions, and then discuss applications through examples of exploration of tabular and image datasets.

Praxis: To demonstrate the use of our interaction and visualization techniques, we integrate them in Praxis, an interactive tool for DR-based exploratory analysis. Although design and implementation details of Praxis are out of the scope of this paper, we give a brief description to help the reader follow the rest of the paper.

Praxis' user interface has four basic elements: *Data Import*, *Selection Details*, *Projection*, and *Data Table*. Through the *Data Import* panel (Figure 6a), users can import a dataset in CSV format, set the projection method (e.g., PCA) using a drop-down selection menu, and view the resulting dimensionality reduction as a scatter plot in the *Projection* plane (Figure 6b). As customary, Praxis uses the first two reduced dimensions (e.g., the first two principal components for PCA) as axes.

The results of forward and backward projection, along with the two visualizations prolines and feasibility map, are displayed in the *Projection* plane. The id (name) of a data point is shown on mouse hover, while clicking performs selection, showing its feature values in the *Selection Details* panel, a dedicated sidebar(Figure 6c). The *Selection Details* panel is used to perform forward projections (clicking on a dimension makes its value modifiable) and to inspect changes in feature values when backward projection is used. The three buttons next to the feature column in this panel respectively 1) reset the feature to its initial value, 2) toggle the inequality constraints on the feature, and 3) lock the feature value to the current—modified—value (i.e., toggles the equality constraint).

Double-clicking the row associated with a feature displays a histogram representing its distribution below the selected row, showing some basic statistics (Figure 6d). The current value of the feature is represented by a blue line and a cyan line indicates the distribution mean. Bins of the histogram are colored similarly to prolines: green for increasing values and red for decreasing values with respect to the original feature value. Users can set constraints on the feature through direct manipulation in the histogram visualization. Dragging one of the two black handles lets the user set or unset lower and upper bounds for a feature distribution, thus defining a set of constraints for a specific data point.

Finally, selecting a data point in the *Projection* plane displays two buttons that respectively enable 1) resetting its feature values (and position) to their original value and 2) showing a tooltip on top of its k currently nearest neighbors, in order to facilitate reasoning about similarity with other data samples; this is particularly useful when performing back projection.

We integrate PCA and autoencoder as dimensionality-reduction methods in Praxis. Next we discuss the first application of our framework, PCA.

Application 1: PCA

Principal component analysis (PCA) is one of the most frequently used linear dimensionality-reduction techniques. PCA computes (learns) a linear orthogonal transformation of the empirically centered data into a new coordinate frame in which the axes represent maximal variability. The process is identical to fitting a high-dimensional ellipsoid to the data. The orthogonal axes of the new coordinate frame, which are also the principal axes, are called principal components. To reduce the number of dimensions to two, for example, we

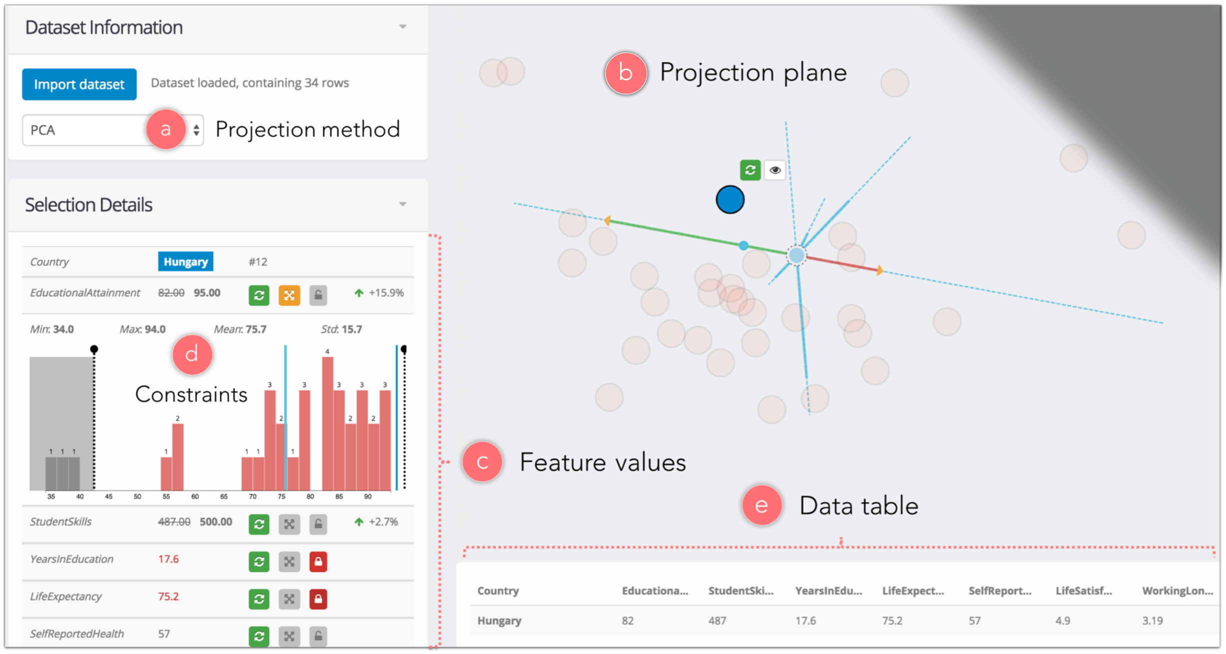

Country	Hungary	#12
EducationalAttainment	~~82.00~~ 95.00	+15.9%
StudentSkills	~~487.00~~ 500.00	+2.7%
YearsInEducation	17.6	
LifeExpectancy	75.2	
SelfReportedHealth	57	

Country	Educationa...	StudentSki...	YearsInEdu...	LifeExpect...	SelfReport...	LifeSatisf...	WorkingLon...
Hungary	82	487	17.6	75.2	57	4.9	3.19

Figure 6: Praxis interface. Praxis is a novel interactive tool for DR-based exploratory data analysis that integrates our visual interactions. After importing a dataset and choosing a projection method (a), a scatter plot is displayed using the two reduced dimensions (b). When a point is selected, its feature values can be seen and modified from a table panel (c) that also allows entering constraints for each feature by double-clicking on a specific row of the table (d). A data table listing all rows in the dataset is also included (e).

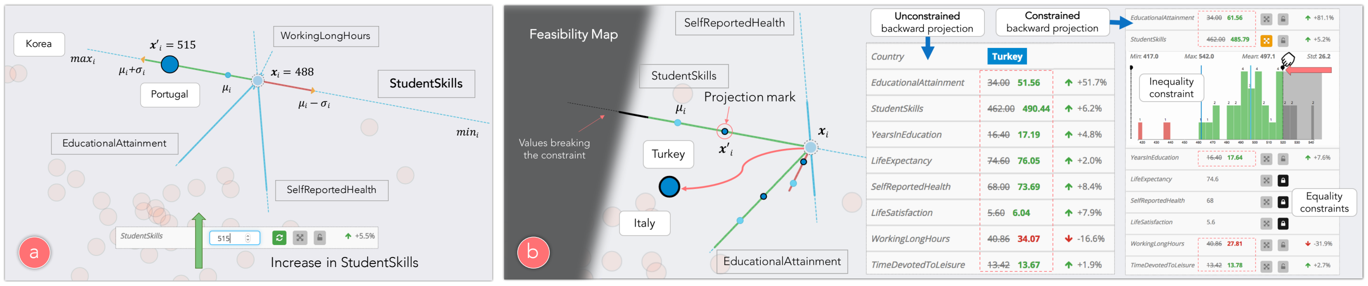

Country	Turkey	
EducationalAttainment	~~34.00~~ 51.56	+51.7%
StudentSkills	~~462.00~~ 490.44	+6.2%
YearsInEducation	~~16.40~~ 17.19	+4.8%
LifeExpectancy	~~74.60~~ 76.05	+2.0%
SelfReportedHealth	~~68.00~~ 73.69	+8.4%
LifeSatisfaction	~~5.60~~ 6.04	+7.9%
WorkingLongHours	~~40.86~~ 34.07	-16.6%
TimeDevotedToLeisure	~~13.42~~ 13.67	+1.9%

EducationalAttainment	~~34.00~~ 61.56	+81.1%
StudentSkills	~~462.00~~ 485.79	+5.2%
YearsInEducation	~~16.40~~ 17.64	+7.6%
LifeExpectancy	74.6	
SelfReportedHealth	68	
LifeSatisfaction	5.6	
WorkingLongHours	~~40.86~~ 27.81	-31.9%
TimeDevotedToLeisure	~~13.42~~ 13.78	+2.7%

Figure 7: PCA-based usage examples with the OECD Better Life dataset. **Left** (a): forward projection with prolines. STUDENTSKILLS is revealed as key feature differentiating Portugal from Korea. Observe that a value of 515 for STUDENTSKILLS would be reasonable with respect to the feature distribution ($\mu_i < 515 < \mu_i + \sigma_i$), but is not enough to make Portugal close to Korea in the projection plane. By visually comparing the lengths (variability) of different proline paths, the user can easily recognize which dimensions contribute most to determining the position of points in the dimensionally reduced space. **Right** (b): backward projection usage. Curious about the projection difference between Turkey and Italy, similar countries in some respects, the user moves the node associated with Turkey (blue circle) towards Italy. Turkey's feature values are automatically updated to satisfy the new projected position as the node is moved. The first table shows how its values would update with unconstrained backward projection, while the second table shows the result of constrained backward projection.

project the centered data matrix, rows of which correspond to data samples and columns to features (dimensions), onto the first two principal components. Details of PCA along with its many formulations and interpretations can be found in standard textbooks on machine learning or data mining (e.g., [7, 25]).

To compute the forward projection change $\Delta\mathbf{y}$ for PCA, we project the data change vector $\Delta\mathbf{x}$ onto the first two principal components: $\Delta\mathbf{y} = \Delta\mathbf{x}\,\mathbf{E}$, where $\Delta\mathbf{x}$ and $\Delta\mathbf{y}$ are row vectors, $\mathbf{E} = [\mathbf{e_0} \quad \mathbf{e_1}]$, and $\mathbf{e_0}$ and $\mathbf{e_1}$ are the first two principal components as column vectors. The formulation of backward projection is the same as for forward projection: $\Delta\mathbf{y} = \Delta\mathbf{x}\,\mathbf{E}$. In this case, however, $\Delta\mathbf{x}$ is unknown and we need to solve the equation.

In the case of unconstrained backward projection, we find $\Delta\mathbf{x}$ by solving a regularized least-squares optimization problem:

$$\begin{aligned} \underset{\Delta\mathbf{x}}{\text{minimize}} \quad & \|\Delta\mathbf{x}\|^2 \\ \text{subject to} \quad & \Delta\mathbf{x}\,\mathbf{E} = \Delta\mathbf{y} \end{aligned}$$

We find a least-norm solution $\Delta\mathbf{x}^*$ by multiplying $\Delta\mathbf{y}$ with the pseudoinverse of $\mathbf{E}$ [9]. This is equivalent to setting $\Delta\mathbf{x}^* = \Delta\mathbf{y}\,\mathbf{E}^T$ as the pseudoinverse of a real-valued orthonormal matrix is equal to the transpose of the matrix.

For constrained backward projection, we find $\Delta\mathbf{x}^*$ by solving the following quadratic optimization problem:

$$\begin{aligned} \underset{\Delta\mathbf{x}}{\text{minimize}} \quad & ||\Delta\mathbf{x}\,\mathbf{E} - \Delta\mathbf{y}||^2 \\ \text{subject to} \quad & \mathbf{C}\Delta\mathbf{x} = \mathbf{d} \\ & \mathbf{lb} \leq \Delta\mathbf{x} \leq \mathbf{ub} \end{aligned}$$

Here $\mathbf{C}$ is the design matrix of equality constraints, $\mathbf{d}$ is the constant vector of equalities, and $\mathbf{lb}$ and $\mathbf{ub}$ are the vectors of lower and upper boundary constraints.

To better understand how these variables are determined, consider a dataset that contains the HEIGHT, WEIGHT, AGE and SCORE values for a set of people. Using the back projection interaction, we would like to experiment with the projection of an individual with the attribute values HEIGHT = 174, WEIGHT = 68, AGE = 30, and SCORE = 8.5. Suppose we constrain AGE to stay fixed (an equality constraint), SCORE to be between 8 and 10, HEIGHT and WEIGHT to be non-negative (inequality constraints) using the Praxis interface. Praxis would set $lb = [-174, -68, -\infty, -0.5]$ and $ub = [+\infty, +\infty, +\infty, 1.5]$ for the inequality constraints. For the equality constraint on AGE, Praxis sets $d = [0,0,30,0]$ and C to be a 4×4 matrix with $[0,0,1,0]$ in its third row and zeros elsewhere.

We now discuss a data exploration facilitated by our visual interactions in which the underlying dimensionality reduction model is PCA. Drawing on earlier work [55], we use the OECD Better Life dataset that contains eight numerical socioeconomic development indices of 34 OECD member countries.

Example: OECD Better Life Index

Zeynep is a data scientist working for a nonprofit organization focusing on economic development. She wants to use the dataset to understand the current situation of various countries in the world and validate her own hypotheses. After importing the dataset into Praxis and choosing PCA as the dimensionality-reduction method, Zeynep observes that the projection plane contains three clearly separated clusters: (1) a large set of westernized (mostly European) countries, (2) Portugal, Turkey, Mexico and Chile, and (3) Korea and Japan. Noticing that Portugal is relatively distant from all other European countries, Zeynep wants to understand which development indices determine its position (Figure 7a). She selects the data point and observes how, of the eight generated prolines, only four of them are long enough to be visible—and they are associated (from the longest to the shortest) to the features STUDENTSKILLS, EDUCATIONALATTAINMENT, SELFREPORTEDHEALTH and WORKINGLONGHOURS. Immediately upon looking at the prolines, Zeynep understands that the remaining four development indices have almost no influence on the current projection, while STUDENTSKILLS (the longest proline) appears to be the most relevant feature. To verify this, she tries to modify the feature value of LIFESATISFACTION and observes that, no matter how large the change, the data point associated to Portugal does not move in the projection plane. On the other hand, slightly changing the value of STUDENTSKILLS moves the point quickly along the associated proline. By observing the direction of each proline, Zeynep understands that features causing Portugal to be distant from the European cluster are EDUCATIONALATTAINMENT and SELFREPORTEDHEALTH, while STUDENTSKILLS seems to be the main feature differentiating it from Korea and Japan. Zeynep now wants to verify if a reasonable increase in STUDENTSKILLS would make Portugal more similar to Korea. While observing the feature distribution information on the associated proline, she sees that Portugal would have to increase STUDENTSKILLS well beyond the maximum value of the distribution.

Zeynep then focuses on another outlier country that has strong historical ties to Europe but has never been part of it: Turkey (Figure 7b). She selects the data point associated to Turkey and drags it towards one of the closest European countries, Italy. Feature values of Turkey are updated through (unconstrained) backward projection (Figure 7b, first table) and Zeynep realizes that the country would have to increase almost all its development indices to become more similar to Italy; only the WORKINGLONGHOURS would have to decrease. While dragging the data point, Zeynep observes from the color of the highlighted prolines that STUDENTSKILLS, SELFREPORTEDHEALTH and EDUCATIONALATTAINMENT are positively intercorrelated (green color), while WORKINGLONGHOURS is negatively correlated (red). Zeynep, wanting to create a more realistic scenario, now assumes the Turkish government cannot directly control indices such as LIFEEXPECTANCY, SELFREPORTEDHEALTH and LIFESATISFACTION, and sets an equality constraint for these features. However, the government can invest a certain amount of money in education, with the plan of increasing the STUDENTSKILLS index to 490 over the next five years. Zeynep sets the inequality constraint on STUDENTSKILLS through a dedicated user interface (Figure 7b, second table). She directly observes from the feasibility map how the region of the projection plane around Italy is reachable given the specified constraints. Then Zeynep again moves Turkey towards Italy through backward projection and observes how this time its feature values are updated to respect the user-defined constraints (Figure 7b, second table). While dragging the point, Zeynep further validates her hypothesis by checking the changing position of projection marks that indicate the current value of each feature with respect to the distribution information encoded on prolines.

Application 2: Autoencoder

In a second application, we demonstrate the framework interactions on autoencoder-based DR. An autoencoder is an artificial neural network model that can learn a low-dimensional representation (or encoding) of data in an unsupervised fashion [48]. Autoencoders using multiple hidden layers with nonlinear activation functions can discover nonlinear mappings between high-dimensional datasets and their low-dimensional representations. Unlike many other DR methods, an autoencoder gives mappings in both directions between the data and low-dimensional (latent) spaces [26], making it a natural candidate for application of the interactions introduced here.

We compute forward projection by performing an encoding pass on the trained autoencoder for a user-modified input. To compute backward projection, we perform a decoding pass on the autoencoder for the user-changed output projection.

For the examples below, we trained an autoencoder model (Figure 8) with six layers of respective sizes (128,32,2,32,128,784) from the first hidden layer to the output layer. Our examples below are from the dimensionality reduction of three image datasets: (1) MNIST handwritten digit database, (2) Google QuickDraw (containing 50 million drawings in 345 different categories), and (3) Fashion MNIST (including images of clothing articles). All three datasets contain 28x28 pixel grayscale images, represented as data vectors of 784 features.

Example: MNIST
Umberto, a data-science student, wants to better understand an autoencoder-based DR of the well-known MNIST dataset. From Praxis, he observes the scatter plot of dimensionally reduced data and notices that similar digits tend to cluster together along different radial directions. He immediately notices an outlier (a "2") within a group of "0"s and wants to understand which key features (pixels) are determining its position in the projection plane (Figure 9a). Hovering on the image with the mouse highlights the prolines associated with each pixels. Umberto observes that lower pixel values at the center of the digit would move the data point down, to within the "0" cluster; conversely, increasing pixel values in the bottom-right corner of the image would move the data point up, towards the other "2"s. He hypothesizes that putting a tail on the digit would make it look more like a "2" and verifies this through forward projection: coloring the appropriate pixels (i.e., increasing their feature values) moves the data point away from the cluster of "0"s.

Umberto now observes how certain regions of the plane are quite dense, while other regions contain very few data samples. He selects a data point from the "0" cluster and drags it into an empty region at the border of the projection plane (Figure 9b). While dragging the point, he observes how the pixel values update, showing alternately features of a "0" and of a "7", the two digits whose clusters are closest to this region of the plane.

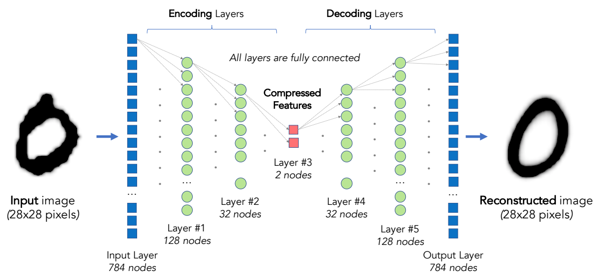

Figure 8: Architecture of the autoencoder trained on the example datasets. The first three hidden layers of the network represent the encoding function, which generates a compressed version of the input image. The last two hidden layers and the output layer represent the decoding function, which aims at reconstructing the original image from its compressed representation.

Example: QuickDraw
Alice, a data scientist, is excited about the recent release of Google Quick Draw dataset and would like to apply DR to a subset (10) of the image categories in the dataset. While performing her analysis with Praxis, she decides to focus on an isolated data point corresponding to the image of an airplane. By filtering its prolines in order to show only the 100 longest ones, Alice can observe which features (pixels) are most influential in determining the position of the image in the projection plane (Figure 9c). In particular, she notices a smaller set of prolines associated to two vertical strips of pixels, suggesting that an increase in their values would move the airplane towards the cluster of beds. Alice decides to perform forward projection and draws two "legs" at the extremes of the airplane: she verifies that the data point has now moved in the "bed" cluster.

Continuing her search for outliers, Alice notices a bed that is apart from the others, probably because it was drawn with only one leg. She wants to see which other images in the dataset may contain a similar shape and uses the brush to define inequality constraints on a set of pixels (Figure 9d): all solutions with pixel values of interest below a specific threshold are not considered acceptable.This way, Alice can directly observe from the admissible region of feasibility map that this particular shape can be found only among bed images.

Example: Fashion MNIST
Mark, an analyst working for a growing apparel company, wants to understand how fashion articles can be better categorized on the company's website on the basis of their image. He uses Praxis to apply autoencoder-based dimensionality reduction on the dataset and notices that the projection plane shows a clear separation of footwear data samples from clothes. The two clusters are set apart by a diagonal group of bags whose images have a distinctive rectangular shape.

Mark wants to explore first the region of the plane containing shoes. He selects a *boot* data sample that appears as an outlier and brings it towards the cluster of points with the same label through backward projection (Figure 9e). Mark notices that the neck of the boot becomes shorter, meaning that the boot's original height was above average. He hypothesizes that the height of a shoe is a critical factor in determining its position in the projection plane. He then drags the same data point close to the cluster of sneakers and watches the pixels of the image modify so that the boot gets even shorter, validating his hypothesis. Moreover, he notices that the boot has become flat, losing its characteristic heel. Finally, wanting to understand what distinguishes sandals from shoes and boots, he continues dragging the data point through backward projection. As he does so, he notices that the pixel density of the image decreases significantly while moving along the main diagonal of the projection plane. Indeed, sandals prove to be the class of images with the fewest colored pixels, because they are open shoes and require less material for construction.

By observing the projection plane, Mark notes that dresses interestingly fall in a region very close to the cluster of trousers. He then selects a dress and observes that many of its (red) prolines are directed towards that cluster, indicating a decrease in pixel values. By hovering these prolines, Mark observes

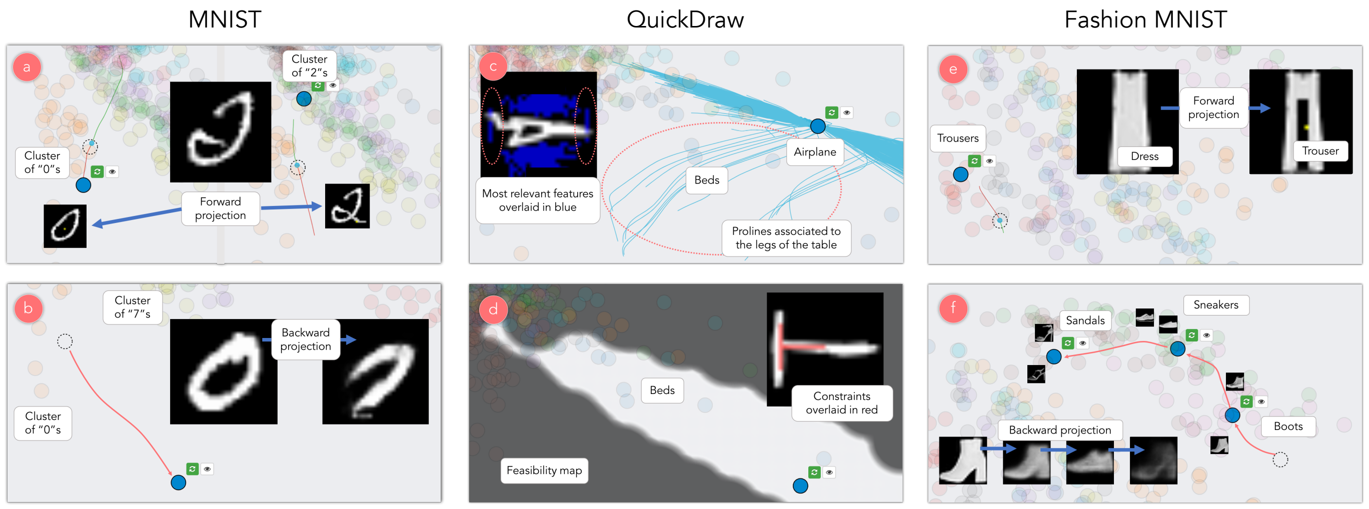

Figure 9: Application of our framework to autoencoder-based data exploration. MNIST: identification of relevant features for an unclear digit through prolines and forward projection (a); exploration of latent space at the borders of the projection plane (b). QuickDraw: prolines show that adding legs to an airplane would make it look more like a bed (c); by setting minimum constraints on the values of a set of pixels (colored in red), the feasibility map shows images similar to the current one (d). Fashion MNIST: the difference between dresses and trousers is explored through forward projection (e); key features differentiating various types of footwear are explored through backward projection (f).

that they correspond to the central region of the dress image. Through forward projection, he erases those pixels (i.e., sets their feature value to zero), making the dress image look like a pair of trousers (Figure 9e). He then observes how the data point quickly moved into the cluster of trousers. Finally, Mark asks himself where a skirt would be positioned in the projection plane if the dataset contained one. So he selects another dress data sample and erases the upper part of its image, shaping a skirt. Noticing how little the data point has moved, he hypothesizes that skirts would cluster with dresses.

DISCUSSION

Scalability and Accuracy

Scalability is a fundamental aspect of any visual interaction technique that can handle large datasets. We design the visual interactions supporting our framework with scalability in mind. Our analysis indicates (Figure 10) that our forward and backward projection implementations for PCA and autoencoder provide a desirable tradeoff between accuracy and speed.

To assess the performance of the framework interactions applied to PCA and autoencoder dimensionality reductions (DRs), we measure the speed and accuracy of forward and backward projections on varying number of data samples and dimensions (see Supplementary Material for details and additional results). For this, we first generate a synthetic dataset by sampling from a multivariate Gaussian distribution with sufficiently large dimensions. We then programmatically induce a change of $\sigma_i/8$ for forward projections and $m/80$ for backward projections, where σ_i is the standard deviation of the ith dimension in the dataset and m is the width of the projection plane. When varying the number of samples, we keep the number of dimensions constant at 10. Conversely, when varying the number of dimensions, we set the number of samples to 100.

Figure 10 (left) suggests that the time required to compute forward and backward projections for interactive applications (~20 microseconds) is not significantly affected by input size. We note that recomputing the DR without out-of-sample extension is several orders of magnitude slower, especially in the case of autoencoder networks.

To measure accuracy, we compute two sets of neighbors on a data point for each performance of our interactions: 1) the k-nearest neighbors in the projection plane after performing a forward or a backward projection and 2) the k-nearest neighbors in the projection plane after recomputing dimensionality reduction on the multidimensional data. We set $k = 10$ for the results shown in Figure 10. Ideally, these two neighborhoods should contain the same elements and the elements should have the same relative distance from the data point on which the interaction is performed. We use a correlation index to quantify the similarity of these two neighborhoods, considering both the number of overlapping elements and the rank order of their distances from the point. Figure 10 (right) shows that the accuracy decreases sublinearly with the input size. On the other hand, the accuracy as measured by our correlation index is either unaffected or slightly improved by the increasing number of dimensions, since the probability of a single attribute change affecting the neighborhood formation and ranking decreases with the increasing number of dimensions.

What about visual scalability? Rendering large number of prolines for high-dimensional datasets can be slow and can clutter the projection view. Sampling and bundling

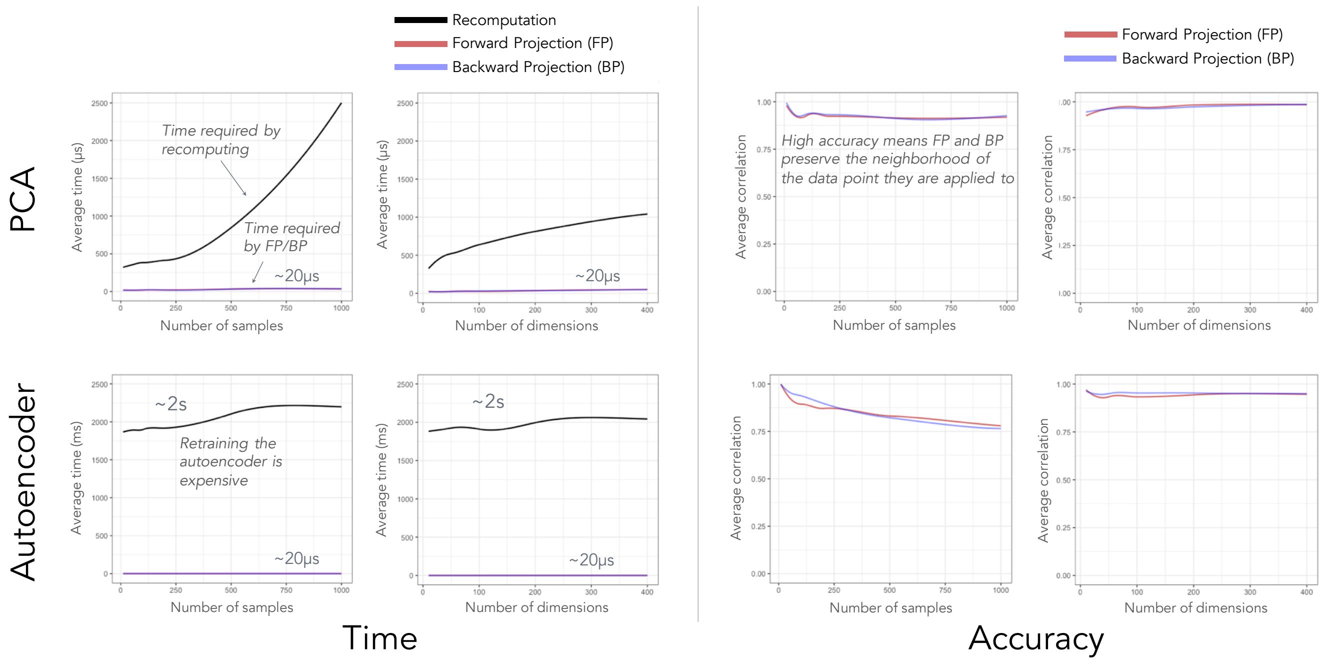

Figure 10: Time and accuracy performance of forward and backward projections for PCA and autoencoder-based dimensionality reductions. Time performance results (left) show how out-of-sample extension outperforms recomputation, guaranteeing low latency even with increasing input size. Accuracy performance results (right) demonstrate how forward and backward projection provide a desirable tradeoff of accuracy and speed.

(aggregation) [17] can help address this problem. Taking a sampling approach, Praxis shows the top-k most "important" prolines when there are too many to draw (Figure 9c).

An important consideration related to accuracy is *trust*. While we focus here on interpretability through dynamic reasoning and experimentation, trust is also an important design criterion for model-based visual analysis [14]. How best to convey the approximation accuracy of our visual interactions to user without degrading computational and visual scalability or inserting additional layer of complexity is an important avenue of future research.

Extending the Framework

Although we focus on DR here, our framework can apply to black-box models in general. Neural network models with multiple hidden layers (or deep neural networks, DNNs) are a particularly popular class of black-box machine learning models, and they have recently achieved dramatic successes. However, formal understanding of these models is limited, and the fact that they can easily have millions of parameters with increasingly intricate architectures only exacerbates the problem. Researchers have recently turned to visualization to gain insights into deep learning models. Prior work applying visualization to improve the understanding and interpretability of deep neural networks shows patterns that fit well in our framework, attesting to its ecological validity and extensibility.

We can group DNN visualization approaches into two broad classes [65]: The first approach is to visualize how the network responds to a specific input in order to explain a particular prediction by the network (e.g.,[4, 40, 42, 53, 54, 62, 63, 64, 65]). A common technique used for convolutional neural networks for computer vision applications is to *occlude* parts of input images and *observe* how the output activation results (e.g., classification) change [62, 63]. This is an instance of a forward projection, changing the input and observing the output change, albeit performed non-interactively in general, with one notable exception [62]. Another common visualization in this approach is saliency maps. Motivated similarly to prolines, saliency maps visualize which features (e.g., pixels) contribute to the output or any other neural unit activation [54, 64, 65].

The second approach is to generate an input that maximally activates a given unit or, say, class score to visualize what the network is looking for in making predictions (e.g.,[21, 35, 36, 45, 54, 62]). Techniques within this approach aim to synthesize input based on a maximization constraint and can be considered an instance of backward projection. DNN researchers also recognize the importance of semantic constraints (e.g., natural image priors) in computing backward projections.

Visualization techniques within the two approaches above have been developed primarily by machine-learning and computer-vision researchers to address their research questions and to understand and communicate the behavior of their models. These techniques are typically computed through command- line interaction and viewed as static images, with limited or no interactivity. Applying dynamic interactions of our framework to DNNs can significantly improve the effectiveness of the visualization techniques DNN researchers already use. A full-fledged integration of backward projection interaction on DNNs, one that interactively changes the activation output of a neural unit and observes the synthesized input, is challenging yet important future work. Crucially, our framework can be useful for orienting future efforts in supporting dynamic reasoning about DNNs. One class of models that would take advantage of our interaction framework is generative and invertible models (e.g., [13, 33, 34, 46]).

Note that black-box models are essential abstractions representing the modularization approach to problem solving. Modularization is effective for allocating human expertise and reducing monetary and cognitive costs, but it decreases controllability and observability. Although contributions from the broader HCI research community are necessary for improving the user experience with machine-learning models, they are not sufficient. Machine-learning models need to be developed with built-in support (analogous to *design for debugging* or *design for testability* in integrated circuit design) for interpretability and explorability in mind. Fortunately, developing interpretable models is of a growing research interest (e.g.,[32, 37, 39, 47]), but much still must be done in this direction, particularly through close collaboration of HCI and machine-learning researchers.

CONCLUSION

We propose a new visual interaction framework that lets users dynamically change the input and output of a dimensionality reduction (DR) and observe the effects of these changes. We achieve this framework through two new interactions, forward projection and backward projection, along with two new visualization techniques, prolines and feasibility map, that facilitate the effective use of the interactions. We apply our framework to principal component analysis (PCA) and autoencoder-based DRs and give examples demonstrating how our visual interactions can improve DR-based data exploration. We show that the framework interactions applied to PCA and autoencoders provide a desirable balance between speed and accuracy to sustain interactivity, scaling gracefully with increasing data size and dimensionality. Finally, we argue that our visual interaction framework can apply to black-box machine learning models at large and discuss how our framework subsumes recent approaches in visualizing deep neural network models.

Exploratory data analysis is an iterative process in which analysts essentially run mental experiments on data, asking questions and (re)forming and evaluating hypotheses. Tukey and Wilk [57] were among the first to observe the similarities between data analysis and doing experiments. Of the eleven similarities between the two that they listed, one in particular is relevant here:"interaction, feedback, trial and error are all essential; convenience is dramatically helpful." In fact, data can be severely underutilized (e.g., *dead* [24, 60]) without what-if analysis. However, to perform data analysis as if we were running data experiments, dynamic visual interactions that bidirectionally bind data and its visual representations must be among our tools. Our work here is a contribution to performing visual analysis in a way similar to running experiments.

ACKNOWLEDGMENTS

The authors thank Paulo Freire for inspiring the name "Praxis."

REFERENCES

1. Elisa Amorim, Emilio V. Brazil, Jesús M.C., Luiz Velho, Luis G. Nonato, Faramarz Samavati, and Mario C. Sousa. 2015. Facing the High-dimensions: Inverse Projection with Radial Basis Functions. *Computers & Graphics* 48 (2015), 35–47.
2. Elisa P.D.S. Amorim, Emilio V. Brazil, Joel Daniels, Paulo Joia, Luis G. Nonato, and Mario C. Sousa. 2012. iLAMP: Exploring High-dimensional Spacing Through Backward Multidimensional Projection. In *Proc. IEEE VAST.*
3. Michael Aupetit. 2007. Visualizing Distortions and Recovering Topology in Continuous Projection Techniques. *Neurocomputing* 70, 7-9 (2007), 1304–1330.
4. Sebastian Bach, Alexander Binder, Grégoire Montavon, Frederick Klauschen, Klaus R. Müller, and Wojciech Samek. 2015. On Pixel-wise Explanations for Non-linear Classifier Decisions by Layer-wise Relevance Propagation. *PloS one* 10, 7 (2015).
5. Benjamin B. Bederson and Angela Boltman. 1999. Does Animation Help Users Build Mental Maps of Spatial Information?. In *Proc. InfoVis*. 28–35.
6. Yoshua Bengio, Jean-François Paiement, Pascal Vincent, Olivier Delalleau, Nicolas Le Roux, and Marie Ouimet. 2003. Out-of-Sample Extensions for LLE, Isomap, MDS, Eigenmaps, and Spectral Clustering. In *NIPS*.
7. Christopher M. Bishop. 2006. *Pattern Recognition and Machine Learning*. Springer-Verlag.
8. Alan Borning. 1981. The Programming Language Aspects of Thinglab, A Constraint-oriented Simulation Laboratory. *ACM TOPLAS* 3, 4 (1981), 353–387.
9. Stephen P. Boyd and Lieven Vandenberghe. 2004. *Convex Optimization*. Cambridge University Press.
10. Matthew Brehmer, Michael Sedlmair, Stephen Ingram, and Tamara Munzner. 2014. Visualizing Dimensionally-reduced Data: Interviews with Analysts and a Characterization of Task Sequences. In *Proc BELIV*.
11. Andreas Buja, Deborah F. Swayne, Michael L. Littman, Nathaniel Dean, Heike Hofmann, and Lisha Chen. 2008. Data Visualization with Multidimensional Scaling. *Journal of Computational and Graphical Statistics* 17, 2 (2008), 444–472.
12. Marco Cavallo and Çağatay Demiralp. 2017. Exploring Dimensionality Reductions with Forward and Backward Projections. In *Proc. Workshop on Interactive Data Exploration and Analytics (IDEA) at KDD*.
13. Xi Chen, Yan Duan, Rein Houthooft, John Schulman, Ilya Sutskever, and Pieter Abbeel. 2016. Infogan: Interpretable Representation Learning by Information Maximizing Generative Adversarial Nets. In *NIPS*. 2172–2180.
14. Jason Chuang, Daniel Ramage, Christopher Manning, and Jeffrey Heer. 2012. Interpretation and Trust: Designing Model-Driven Visualizations for Text Analysis. In *Proc. CHI*.

15. Danilo B. Coimbra, Rafael M. Martins, Tácito T.A.T. Neves, Alexandru C. Telea, and Fernando V. Paulovich. 2016. Explaining Three-dimensional Dimensionality Reduction Plots. *Information Visualization* 15, 2 (2016), 154–172.

16. Tarik Crnovrsanin, Chris Muelder, Carlos Correa, and Kwan-Liu Ma. 2009. Proximity-based Visualization of Movement Trace Data. In *Proc. IEEE VAST*.

17. Renato R.O. da Silva, Paulo E. Rauber, and Alexandru C. Telea. 2016. Beyond the Third Dimension: Visualizing High-dimensional Data with Projections. *Computing in Science & Engineering* 18, 5 (2016), 98–107.

18. Çağatay Demiralp. 2016. Clustrophile: A Tool for Visual Clustering Analysis. In *KDD IDEA*.

19. Alex Endert, Patrick Fiaux, and Chris North. 2012. Semantic Interaction for Visual Text Analytics. In *Proc. CHI*.

20. Alex Endert, Chao Han, Dipayan Maiti, Leanna House, and Chris North. 2011. Observation-level Interaction With Statistical Models for Visual Analytics. In *Proc. IEEE VAST*.

21. Dumitru Erhan, Yoshua Bengio, Aaron Courville, and Pascal Vincent. 2009. *Visualizing Higher-Layer Features of a Deep Network*. Technical Report 1341. University of Montreal.

22. Karl Ruben Gabriel. 1971. The Biplot Graphic Display of Matrices with Application to Principal Component Analysis. *Biometrika* (1971), 453–467.

23. Michael Gleicher. 2013. Explainers: Expert Explorations with Crafted Projections. *IEEE TVCG* 19, 12 (2013), 2042–2051.

24. Peter J. Haas, Paul P. Maglio, Patricia G. Selinger, and Wang C. Tan. 2011. Data is Dead... Without What-if Models. *PVLDB* 4, 12 (2011), 1486–1489.

25. Trevor Hastie, Robert Tibshirani, Jerome Friedman, and James Franklin. 2005. The Elements of Statistical Learning: Data Mining, Inference and Prediction. *The Mathematical Intelligencer* 27, 2 (2005), 83–85.

26. Geoffrey E. Hinton and Ruslan R. Salakhutdinov. 2006. Reducing the Dimensionality of Data with Neural Networks. *Science* 313, 5786 (2006), 504–507.

27. Edwin L. Hutchins, James D. Hollan, and Donald A. Norman. 1985. Direct Manipulation Interfaces. *Human–Computer Interaction* 1, 4 (1985), 311–338.

28. Dong H. Jeong, Caroline Ziemkiewicz, Brian Fisher, William Ribarsky, and Remco Chang. 2009. iPCA: An Interactive System for PCA-based Visual Analytics. *Computer Graphics Forum* 28, 3 (2009), 767–774.

29. Sara Johansson and Jimmy Johansson. 2009. Interactive Dimensionality Reduction Through User-defined Combinations of Quality Metrics. *IEEE TVCG* 15, 6 (2009), 993–1000.

30. Paulo Joia, Danilo Coimbra, Jose A. Cuminato, Fernando V. Paulovich, and Luis G. Nonato. 2011. Local Affine Multidimensional Projection. *IEEE TVCG* 17, 12 (2011), 2563–2571.

31. Alan Kay and Adele Goldberg. 1977. Personal Dynamic Media. *Computer* 10, 3 (1977), 31–41.

32. Been Kim, Julie A. Shah, and Finale Doshi-Velez. 2015. Mind the Gap: A Generative Approach to Interpretable Feature Selection and Extraction. In *NIPS*. 2260–2268.

33. Diederik P. Kingma and Max Welling. 2013. Auto-encoding Variational Bayes. *arXiv preprint arXiv:1312.6114* (2013).

34. Guillaume Lample, Neil Zeghidour, Nicolas Usunier, Antoine Bordes, Ludovic Denoyer, and Marc'Aurelio Ranzato. 2017. Fader Networks: Manipulating Images by Sliding Attributes. *arXiv preprint arXiv:1706.00409* (2017).

35. Quoc V. Le, Marc'Aurelio Ranzato, Rajat Monga, Matthieu Devin, Kai Chen, Greg S. Corrado, Jeff Dean, and Andrew Y. Ng. 2012. Building High-level Features Using Large Scale Unsupervised Learning. In *Proc. ICML*.

36. Honglak Lee, Chaitanya Ekanadham, and Andrew Y. Ng. 2007. Sparse Deep Belief Net Model for Visual Area V2. In *NIPS*.

37. Tao Lei, Regina Barzilay, and Tommi Jaakkola. 2016. Rationalizing Neural Predictions. *Proc. EMNLP* (2016).

38. Sylvain Lespinats and Michael Aupetit. 2010. CheckViz: Sanity Check and Topological Clues for Linear and Non-Linear Mappings. *Computer Graphics Forum* 30, 1 (2010), 113–125.

39. Benjamin Letham, Cynthia Rudin, Tyler H. McCormick, David Madigan, and others. 2015. Interpretable Classifiers Using Rules and Bayesian Analysis: Building a Better Stroke Prediction Model. *The Annals of Applied Statistics* 9, 3 (2015), 1350–1371.

40. Jiwei Li, Xinlei Chen, Eduard Hovy, and Dan Jurafsky. 2015. Visualizing and Understanding Neural Models in NLP. *arXiv preprint arXiv:1506.01066* (2015).

41. Laurens van der Maaten and Geoffrey Hinton. 2008. Visualizing Data Using t-SNE. *Journal of Machine Learning Research* 9 (2008), 2579–2605.

42. Aravindh Mahendran and Andrea Vedaldi. 2015. Understanding Deep Image Representations by Inverting Them. In *CVPR*.

43. Gladys M.H. Mamani, Francisco M. Fatore, Luis G. Nonato, and Fernando V. Paulovich. 2013. User-driven Feature Space Transformation. *Computer Graphics Forum* 32 (2013), 291–299.

44. Nathan D. Monnig, Bengt Fornberg, and Francois G. Meyer. 2014. Inverting Nonlinear Dimensionality Reduction with Scale-free Radial Basis Function Interpolation. *Applied and Computational Harmonic Analysis* 37, 1 (2014), 162–170.

45. Anh Nguyen, Jason Yosinski, and Jeff Clune. 2016. Multifaceted Feature Visualization: Uncovering the Different Types of Features Learned by Each Neuron in Deep Neural Networks. (2016).

46. Guim Perarnau, Joost van de Weijer, Bogdan Raducanu, and Jose M. Álvarez. 2016. Invertible Conditional GANs for Image Editing. *arXiv preprint arXiv:1611.06355* (2016).

47. Marco T. Ribeiro, Sameer Singh, and Carlos Guestrin. 2016. Why Should I Trust you?: Explaining the Predictions of Any Classifier. In *Proc. KDD*. ACM, 1135–1144.

48. David E. Rumelhart, Geoffrey. E. Hinton, and Ronald. J. Williams. 1986. In *Parallel Distributed Processing: Explorations in the Microstructure of Cognition, Vol. 1*, David E. Rumelhart and James L. McClelland (Eds.). Chapter Learning Internal Representations by Error Propagation, 318–362.

49. Dominik Sacha, Leishi Zhang, Michael Sedlmair, John A. Lee, Jaakko Peltonen, Daniel Weiskopf, Stephen C. North, and Daniel A. Keim. 2017. Visual Interaction with Dimensionality Reduction: A Structured Literature Analysis. *IEEE TVCG* 23, 1 (2017), 241–250.

50. Tobias Schreck, Jurgen Bernard, Tatiana von Landesberger, and Jorn Kohlhammer. 2009. Visual Cluster Analysis of Trajectory Data with Interactive Kohonen Maps. *Information Visualization* 8, 1 (2009), 14–29.

51. Michael Sedlmair, Tamara Munzner, and Melanie Tory. 2013. Empirical Guidance on Scatterplot and Dimension Reduction Technique Choices. *IEEE TVCG* 19, 12 (2013), 2634–2643.

52. Ben Shneiderman. 1983. Direct Manipulation: A Step Beyond Programming Languages. *Computer* 16, 8 (1983), 57–69.

53. Avanti Shrikumar, Peyton Greenside, Anna Shcherbina, and Anshul Kundaje. 2016. Not Just a Black Box: Learning Important Features Through Propagating Activation Differences. *arXiv preprint arXiv:1605.01713* (2016).

54. Karen Simonyan, Andrea Vedaldi, and Andrew Zisserman. 2013. Deep Inside Convolutional Networks: Visualising Image Classification Models and Saliency Maps. (2013).

55. Julian Stahnke, Marian Dörk, Boris Müller, and Andreas Thom. 2016. Probing Projections: Interaction Techniques for Interpreting Arrangements and Errors of Dimensionality Reductions. *IEEE TVCG* 22, 1 (2016), 629–638.

56. Ivan E. Sutherland. 1963. Sketchpad: A Man-machine Graphical Communication System. In *Proc. Spring Joint Computer Conference*.

57. John W. Tukey and Martin B. Wilk. 1966. Data Analysis and Statistics: An Expository Overview. In *Proc. Fall Joint Computer Conference*.

58. Laurens van der Maaten, Eric Postma, and Japp van den Herik. 2009. *Dimensionality Reduction: A Comparative Review*. Technical Report. TiCC, Tilburg University.

59. Christophe Viau, Michael J. McGuffin, Yves Chiricota, and Igor Jurisica. 2010. The FlowVizMenu and Parallel Scatterplot Matrix: Hybrid Multidimensional Visualizations for Network Exploration. *IEEE TVCG* (2010), 1100–1108.

60. Bret Victor. 2013. Media for Thinking the Unthinkable. `https://vimeo.com/67076984`. (2013). Accessed: Dec 24th, 2017.

61. Matt Williams and Tamara Munzner. 2004. Steerable, Progressive Multidimensional Scaling. In *Proc. IEEE InfoVis*.

62. Jason Yosinski, Jeff Clune, Anh Nguyen, Thomas Fuchs, and Hod Lipson. 2015. Understanding Neural Networks Through Deep Visualization. (2015).

63. Matthew D. Zeiler and Rob Fergus. 2014. Visualizing and Understanding Convolutional Networks. In *Proc. ECCV*.

64. Bolei Zhou, Aditya Khosla, Agata Lapedriza, Aude Oliva, and Antonio Torralba. 2016. Learning Deep Features for Discriminative Localization. In *CVPR*.

65. Luisa M. Zintgraf, Taco S. Cohen, Tameem Adel, and Max Welling. 2017. Visualizing Deep Neural Network Decisions: Prediction Difference Analysis. In *Proc. ICLR*.